VIP Heterogeneous Catalysis Very Important Paper

International Edition: DOI: 10.1002/anie.201601208
German Edition: DOI: 10.1002/ange.201601208

Direct and Highly Selective Conversion of Synthesis Gas into Lower Olefins: Design of a Bifunctional Catalyst Combining Methanol Synthesis and Carbon–Carbon Coupling

Kang Cheng[+], *Bang Gu*[+], *Xiaoliang Liu*[+], *Jincan Kang*, *Qinghong Zhang*,* *and Ye Wang**

Abstract: *The direct synthesis of lower (C_2 to C_4) olefins, key building-block chemicals, from syngas (H_2/CO), which can be derived from various nonpetroleum carbon resources, is highly attractive, but the selectivity for lower olefins is low because of the limitation of the Anderson–Schulz–Flory distribution. We report that the coupling of methanol-synthesis and methanol-to-olefins reactions with a bifunctional catalyst can realize the direct conversion of syngas to lower olefins with exceptionally high selectivity. We demonstrate that the choice of two active components and the integration manner of the components are crucial to lower olefin selectivity. The combination of a Zr–Zn binary oxide, which alone shows higher selectivity for methanol and dimethyl ether even at 673 K, and SAPO-34 with decreased acidity offers around 70 % selectivity for C_2–C_4 olefins at about 10 % CO conversion. The micro- to nanoscale proximity of the components favors the lower olefin selectivity.*

Lower olefins are key building-block chemicals. Currently, lower olefins are produced primarily by thermal cracking of naphtha. The growing demand for lower olefins and the depletion of oil reserves have stimulated the development of processes for lower olefin synthesis from alternative feedstocks such as coal, natural gas (also shale gas), and biomass.[1] Synthesis gas (syngas, CO/H_2) is a key platform for the transformation of nonpetroleum carbon resources. The synthesis of lower olefins from syngas is a promising route.

Many studies have been devoted to the hydrogenation of CO to lower olefins by Fischer–Tropsch (FT) synthesis over Fe catalysts.[1–5] However, the selectivity for C_2–C_4 olefins is limited. Typically, FT synthesis proceeds by the dissociation of CO, formation of CH_x ($x = 1$–3), coupling of CH_x to C_nH_m, and the hydrogenation or dehydrogenation of C_nH_m to paraffin or olefin products.[1] The coupling of CH_x is uncontrollable over metal catalysts (Fe, Co, and Ru) capable of catalyzing CO dissociation, and thus the hydrocarbon products generally follow a statistical distribution known as the Anderson–Schulz–Flory (ASF) distribution.[1] According to this distribution, the maximum C_2–C_4 (including paraffins and olefins) selectivity is limited to 58 %. Recently, a C_2–C_4 olefin selectivity of approximately 60 % was achieved through careful design of catalysts containing S- and Na-modified Fe nanoparticles dispersed on weakly interactive supports.[2]

Lower olefins can also be produced from syngas by two consecutive processes, namely methanol synthesis and methanol to olefins (MTO).[6] Compared to the two-process route, the direct route would be more energy- and cost-efficient. A direct route that employs bifunctional catalysts capable of catalyzing the CO hydrogenation to heavier hydrocarbons and the selective C−C cleavage of heavier hydrocarbons has been reported to be effective for the production of gasoline or diesel fuel.[7] We expect that the development of a bifunctional catalyst containing active components for the conversion of CO to C_1 intermediates (e.g., CH_3OH or CH_3O) and the selective C−C coupling would be a promising strategy to realize the selective conversion of syngas to C_2–C_4 olefins (Figure 1). Carrying out C−C coupling and CO activation on different sites may allow the coupling to proceed in a controlled manner, thus breaking the ASF distribution. Some studies have combined methanol synthesis and methanol-to-hydrocarbon catalysts in one reactor, but the major products are C_2–C_4 paraffins.[8] The direct synthesis of C_2–C_4 olefins from syngas with high selectivity (> 60 %) is a big challenge. Herein, we report a successful design of bifunctional catalysts with exceptionally high selectivity for C_2–C_4 olefins by integrating catalyst components that are active in methanol synthesis and in C−C coupling. We demonstrate that the choice of the components and their integration are crucial to the product selectivity.

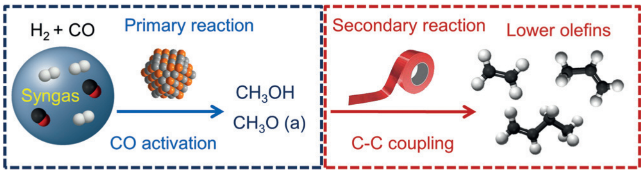

Figure 1. Reaction coupling for the direct synthesis of lower olefins from syngas by the integration of active components for CO activation and C−C coupling. (a) = adsorbed.

We chose molecular sieve SAPO-34, an excellent MTO catalyst,[6] as the C−C coupling component. The optimized temperature for SAPO-34-catalyzed C_2–C_4 olefin synthesis is 673–723 K.[6] However, methanol synthesis at such high

---

[*] Dr. K. Cheng,[+] B. Gu,[+] X. Liu,[+] Dr. J. Kang, Prof. Dr. Q. Zhang, Prof. Dr. Y. Wang
State Key Laboratory of Physical Chemistry of Solid Surfaces
Collaborative Innovation Center of Chemistry for Energy Materials
National Engineering Laboratory for Green Chemical Productions of Alcohols, Ethers and Esters
College of Chemistry and Chemical Engineering, Xiamen University
Xiamen 361005 (China)
E-mail: zhangqh@xmu.edu.cn
wangye@xmu.edu.cn

[+] These authors contributed equally to this work.

Supporting information and the ORCID identification number(s) for the author(s) of this article can be found under http://dx.doi.org/10.1002/anie.201601208.

temperatures is thermodynamically restrained (See Figure S1 in the Supporting Information). Our calculations show that the coupling with the MTO reaction, which is thermodynamically more feasible at higher temperatures, can drive the conversion of syngas and the formation of lower olefins is thermodynamically feasible at 673 K (Figure S1). We first used ball-milling to combine a typical methanol synthesis catalyst, namely Cu–Zn–Al mixed oxide, with SAPO-34 for syngas conversion. The Cu–Zn–Al catalyst alone exhibited high selectivity for the production of methanol at 523 K, but the major product shifted to CH_4 as the temperature rose to 673 K (Table 1), thus indicating that the hydrogenolysis of the C−O bond occurred at such a high temperature. Methanol was mostly converted to dimethyl ether (DME) over the Cu–Zn–Al/SAPO-34 composite at 523 K, thus suggesting that SAPO-34 catalyzed the intermolecular dehydration of methanol under such conditions. At 673 K, the C−C coupling products, C_2–C_4 paraffins, were formed along with CH_4 over this catalyst, but the C_2–C_4 olefin selectivity was very low. CO_2 was also formed with a selectivity of around 45 % over the Cu–Zn–Al or Cu–Zn–Al/SAPO-34 catalyst at 673 K because of the water–gas-shift (WGS) reaction (Table S1). Similar results were observed when SAPO-34 was integrated with several other methanol synthesis catalysts such as Pd–Zn and Cr–Zn (Table S2) that have been previously reported.[8] Distinct from these results, we discovered that a bifunctional catalyst composed of Zr–Zn binary oxide and SAPO-34 is unique for the formation of C_2–C_4 olefins (Table 1). The C_2–C_4 olefin selectivity reached 63 % with CO conversion of 9.5 % at 673 K over the Zr–Zn/SAPO-34 catalyst with a Zr/Zn molar ratio of 2:1. Unlike the Cu–Zn–Al catalyst, methanol and DME remained as the major products over the Zr–Zn catalyst over a wide temperature range (Figure S2). The CO conversion was lower over the Zr–Zn catalyst, but the coupling with SAPO-34 significantly accelerated the conversion at 673 K because of the thermodynamic driving force.

Table 1: Hydrogenation of CO over methanol synthesis catalysts and bifunctional catalysts composed of methanol synthesis catalyst and SAPO-34.[a]

Catalyst[b]	CO conv. [%]	Selectivity for CO hydrogenation[c] [%]				
		CH_4	$C_{2-4}^{=}$	C_{2-4}^{0}	C_{5+}	CH_3OH (DME)
Cu–Zn–Al[d]	6.3	0.3	0.3	1.9	1.0	96(0.8)
Cu–Zn–Al	5.7	86	0.1	9.1	0	3.8(0.8)
Cu–Zn–Al/SAPO-34[d]	4.8	0.1	0	0.1	0	8.0(92)
Cu–Zn–Al/SAPO-34	10	9.3	1.2	86	3.7	0(0)
Zr–Zn(2:1)[d]	0.2	0.1	0.1	0.1	0.8	98(0.7)
Zr–Zn(2:1)	1.1	19	9.3	3.3	3.4	25(40)
Zr–Zn(2:1)/SAPO-34[d]	0.1	1.1	4.6	2.4	2.0	29(61)
Zr–Zn(2:1)/SAPO-34	9.5	6.0	63	29	2.2	0(0)
ZrO_2	0.3	4.6	11	2.8	1.0	80(0.8)
ZrO_2/SAPO-34	1.0	4.0	90	5.5	1.1	0(0)
Zr–Zn(4:1)	0.8	7.9	2.6	0.5	1.2	54(33)
Zr–Zn(4:1)/SAPO-34	6.8	4.2	69	25	2.1	0(0)
Zr–Zn(1:1)	1.4	35	5.8	5.2	3.1	19(31)
Zr–Zn(1:1)/SAPO-34	7.5	11	37	48	3.2	0(0)
ZnO	1.8	84	4.4	6.5	0.5	4.7(0.2)
ZnO/SAPO-34	3.3	43	8.1	49	0	0(0)

[a] Reaction conditions: catalyst 0.50 g; $H_2/CO = 2:1$; 1 MPa; 30 mL min^{-1}; time on stream 30 h; 673 K. [b] Cu/Zn/Al = 6:3:1 (molar ratio); the Zr/Zn molar ratio is shown in the parentheses; the composites were prepared by ball-milling for 24 h. [c] Selectivity was calculated on a molar carbon basis for CO hydrogenation; the formation of CO_2 by the WGS reaction was shown in Table S1; $C_{2-4}^{=}$, C_{2-4}^{0}, and C_{5+} denote C_2–C_4 olefins, C_2–C_4 paraffins, and hydrocarbons with carbon numbers greater than 5, respectively. [d] 523 K.

We performed further studies to understand the unique catalytic functions of the Zr–Zn-based catalysts. Use of ZrO_2 alone provided CH_3OH with a high selectivity, but CO conversion was low (Table 1). The ZrO_2/SAPO-34 composite exhibited a C_2–C_4 olefin selectivity of 90 % at CO conversion of 1.0 %. The high olefin selectivity is likely due to the weak hydrogenation ability of ZrO_2. Actually, ZrO_2 is a unique catalyst in CO activation with surface oxygen vacancies, and forms surface methoxide via formate in the presence of H_2.[9] However, the ability of ZrO_2 to dissociate H_2 is low, thus resulting in its low activity even in combination with SAPO-34. The presence of a second component that can accelerate dissociative H_2 adsorption would favor the CO conversion over ZrO_2. ZnO is well known to function in the heterolytic dissociation of H_2, forming hydrogen species capable of participating in hydrogenation reactions.[10] The results in Table 1 suggest that ZnO activates H_2 in our system, thus enhancing the hydrogenation of CO over the Zr–Zn/SAPO-34 catalyst. The catalyst with a Zr/Zn molar ratio of 2:1 exhibited the highest activity for C_2–C_4 olefin formation. A higher Zn/Zr ratio led to higher CH_4 selectivity and C_2–C_4 paraffin/olefin ratio because of the higher hydrogenation ability. Characterization by using XRD and TEM confirmed that the Zr–Zn binary oxide was composed of nanosized ZrO_2 and ZnO particles (Figures S3 and S4).

Our results suggest that the CO hydrogenation active component significantly affects the product selectivity in the subsequent conversion of methanol or the methoxide intermediate. We performed methanol conversion in the presence of H_2 at 673 K to gain more insights. The methanol conversion was greater than 98 % over the catalysts displayed in Figure 2. C_2–C_4 olefins and paraffins were formed as the major products over SAPO-34, which had been ball-milled for 24 h for a better comparison and is denoted as SAPO-34(24h). The presence of ZrO_2 did not significantly affect the product selectivity. The increase in the Zn/Zr ratio in Zr–Zn/SAPO-34 composites gradually increased CH_4 selectivity. The C_2–C_4 olefin/paraffin ratio decreased at the same time. Only C_2–C_4 paraffins were formed over the Cu–Zn–Al/SAPO-34 catalyst. These trends are similar to those observed for syngas conversion (Table 1) and can explain why the Zr–Zn/SAPO-34 is unique for C_2–C_4 olefin formation. Thus, the choice of a CO hydrogenation active component with appropriate hydrogenation ability is quite important for the selective formation of C_2–C_4 olefins.

It is noteworthy that the C_2–C_4 olefin/paraffin ratios for some catalysts were lower for methanol conversion under H_2 (Figure 2) than those for syngas conversion (Table 1) and those reported for the MTO reaction.[6] We clarified that this behavior arises from the effect of the presence of H_2 or the difference in H_2 pressure. Under the N_2 atmosphere typically

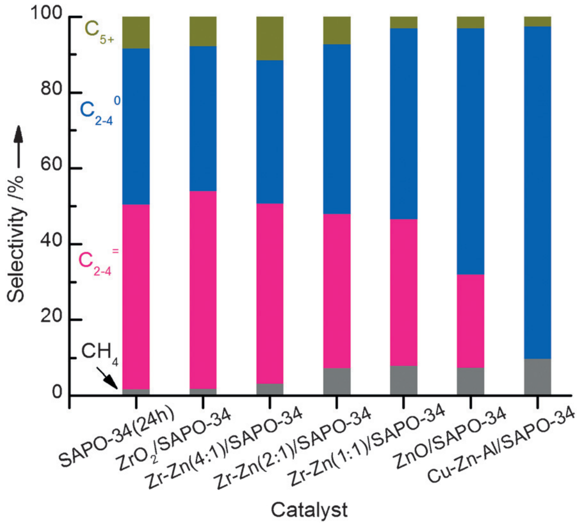

Figure 2. Influence of the CO hydrogenation active component on the conversion of methanol under H_2. All the catalysts were prepared by ball-milling for 24 h. Reaction conditions: catalyst 0.50 g, 673 K; H_2 1.0 MPa, 30 mL min^{-1}; liquid methanol 0.010 mL min^{-1}; time on stream 200 min.

used for the MTO reaction, the C_2–C_4 olefin selectivity reached around 80% over SAPO-34(24h) (Figure S5). The increase in H_2 pressure resulted in a decreased selectivity for C_2–C_4 olefins and increased selectivity for C_2–C_4 paraffins because of the hydrogenation over the Brønsted acid sites of SAPO-34.[11] For the same reason, the increase in syngas pressure from 1.0 to 2.0 MPa decreased the C_2–C_4 olefin/paraffin ratio in syngas conversion over the Zr–Zn/SAPO-34 catalyst (Table S3).

Because the hydrogenation of olefins can occur on the Brønsted acid sites, the acidity of SAPO-34 may also affect the product selectivity. We found that the ball-milling decreased the crystal size (Figure S6), the crystallinity (Figure S7a), and the specific surface area (Table S4) of SAPO-34. The coordination environments of Si, Al, and P in SAPO-34 were also altered at the same time (Figure S8). It is known that the Brønsted acidity of SAPO-34 arises from the substitution of Si for P or Al in the framework.[6] Thus, the change in the coordination environment may lead to the change in Brønsted acidity. Our NH_3 temperature-programmed desorption (NH_3-TPD) studies showed that the density of Brønsted acid sites decreased with an increase in the ball-milling time (Figure S9a and Table S4). We also studied a series of SAPO-34 samples with different Si contents [$x = Si/(Si+Al+P)$] (Table S4), which were denoted as SAPO-34(Six) and had good crystallinity (Figure S7b), and thus different densities of Brønsted acid sites (Figure S9b and Table S4). The results for methanol conversion under H_2 with these two series of SAPO-34 samples demonstrate that the density of Brønsted acid sites is a key factor that determines the C_2–C_4 olefin/paraffin ratio (Figure 3a). A larger density of Brønsted acid sites resulted in a lower olefin/paraffin ratio or lower C_2–C_4 olefin selectivity. Similar trends were observed for syngas conversion over bifunctional catalysts prepared by a simple mixing in an agate mortar of the Zr–Zn (Zn/Zr = 1:2) oxide and SAPO-34 samples with different densities of Brønsted acid sites (Figure 3b). A C_2–C_4 olefin selectivity of 74% was obtained at CO conversion of 11% over the Zr–Zn/SAPO-34(Si0.048)-M (M = mortar-mixing) catalyst with a density of Brønsted acid sites of 0.21 mmol g^{-1}.

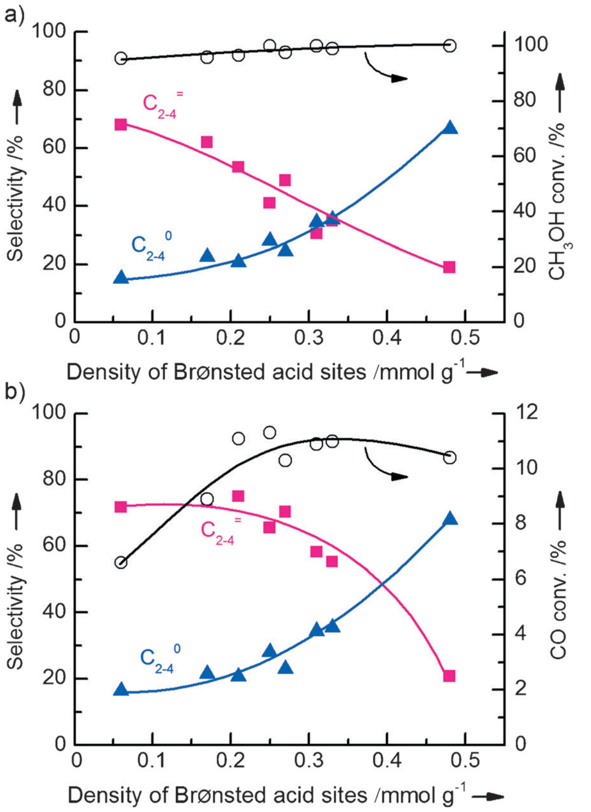

Figure 3. Effect of Brønsted acidity of SAPO-34 on catalytic behavior. a) Methanol conversion over SAPO-34 with different acidities under reaction conditions shown in Figure 2. b) Syngas conversion over composite catalysts prepared by simple mixing in an agate mortar of Zr–Zn (Zr/Zn = 2:1) oxide and SAPO-34 with different acidities under reaction conditions given in Table 1.

The integration manner of the active components is also crucial for the conversion of syngas to lower olefins. The use of a dual-bed configuration with SAPO-34(24h) downstream from the Zr–Zn oxide provided a very low CO conversion (Figure 4a). This result suggests that the thermodynamic driving force does not arise from separating the two active components. The CH_4 selectivity remained high, but C_2–C_4 olefins and paraffins were formed because of the catalytic function of SAPO-34 in the downstream bed. The mixing of the two components significantly increased CO conversion and decreased CH_4 selectivity (Figure 4b–d). The proximity of the two components increased as the integration manner changed from granule-stacking to ball-milling (Figure 4b to 4d), as demonstrated by the electron microscopy results (Figures S10–S13). For the typical Zr–Zn/SAPO-34 sample with the two components ball-milled together for 24 h (Figure 4d), the smaller Zr–Zn particles (10–40 nm) were tightly attached on SAPO-34 particles with sizes of 200–500 nm (Figures S12 and S13). On the other hand, the contact between the SAPO-34 particles with sizes of 200–500 nm and

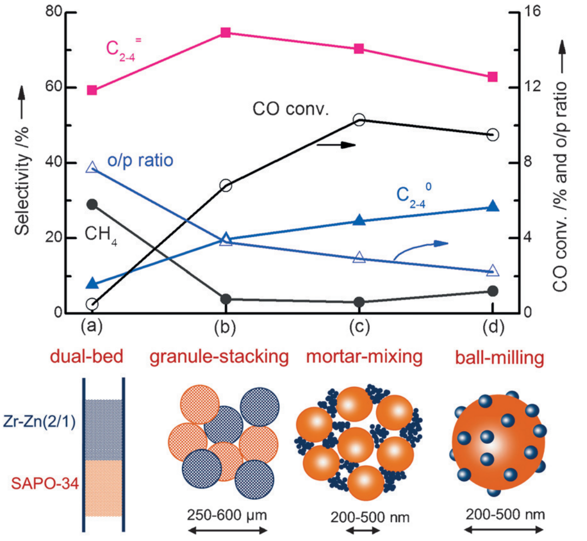

Figure 4. Effect of integration manner on catalytic behaviors of the composite catalysts containing Zr–Zn (Zr/Zn = 2:1) oxide and SAPO-34(24 h). a) Dual-bed configuration. b) Stacking of granules with sizes of 250–600 μm. c) Simple mixing of the two components in an agate mortar. d) Ball-milling of two components together for 24 h. o/p ratio denotes the C_2–C_4 olefin/paraffin ratio. See Table 1 for reaction conditions.

the irregular Zr–Zn particles was not very tight (Figure S11) in the sample prepared by simple mixing of ball-milled SAPO-34 and Zr–Zn particles in an agate mortar (Figure 4c). The sample represented in Figure 4b was composed of micrometer-sized particles stacked together (Figure S10). CO conversion of around 10% was obtained over the catalysts with nanoscale dimensions (Figure 4c,d). The selectivity for C_2–C_4 olefins decreased and that for C_2–C_4 paraffins increased slightly with an increase in the proximity of the two components (Figures 4b–d). Recently, de Jong and co-workers reported that overly tight contact of bifunctional active sites was detrimental to the hydrocracking of hydrocarbons.[12] In our case, the increase in the proximity may increase the probability of unfavorable hydrogenation of the target lower olefins formed on SAPO-34 by the nearby Zr–Zn oxides. We have further measured the stability of the composite of Figure 4c. The changes in both CO conversion and product selectivity were not significant after 20 h of reaction (Figure S14). The conversion of CO and the selectivity of C_2–C_4 olefins were sustained at 9.2% and 68%, respectively, after 100 h of reaction. Thus, the present composite catalyst is quite stable for the direct conversion of CO to lower olefins.

In conclusion, we have discovered that the integration of the Zr–Zn binary oxide, which is responsible for the activation of CO to methanol or methoxide, and SAPO-34 responsible for the selective C–C coupling can realize the direct synthesis of lower olefins from syngas with excellent selectivity. The C_2–C_4 olefin selectivity can reach 74% with a CO conversion of 11% at 673 K, thus breaking the ASF distribution. We have demonstrated that the control of the hydrogenation ability of the two components in the bifunctional catalyst is crucial to obtaining high C_2–C_4 olefin selectivity. The proximity of the two components also plays a key role in the direct conversion of syngas to lower olefins.

Experimental Section

The Zr–Zn binary oxide was prepared by a coprecipitation method. The Zr–Zn/SAPO-34 composites with a mass ratio of the two components of 1:2 were typically prepared by ball-milling for 24 h. The conversion of syngas was performed in a fixed-bed reactor using syngas (H_2/CO = 2:1) with a pressure of 1.0 MPa at 673 K. The conversion of methanol was performed in the same reactor under H_2 (1.0 MPa). See the Supporting Information for experimental details.

Acknowledgements

This work was supported by the National Basic Research Program of China (2013CB933102), the Natural Science Foundation of China (91545203, 21433008 and 21503174), and the China Postdoctoral Science Foundation (2015M571967).

Keywords: bifunctional catalysts · C–C coupling · heterogeneous catalysis · synthesis gas · zeolites

How to cite: *Angew. Chem. Int. Ed.* **2016**, *55*, 4725–4728
Angew. Chem. **2016**, *128*, 4803–4806

---

[1] H. M. Torres Galvis, K. P. de Jong, *ACS Catal.* **2013**, *3*, 2130–2149.
[2] H. M. Torres Galvis, J. H. Bitter, C. B. Khare, M. Ruitenbeek, A. I. Dugulan, K. P. de Jong, *Science* **2012**, *335*, 835–838.
[3] X. Chen, D. Deng, X. Pan, Y. Hu, X. Bao, *Chem. Commun.* **2015**, *51*, 217–220.
[4] J. Lu, L. Yang, B. Xu, Q. Wu, D. Zhang, S. Yuan, Y. Zhai, X. Wang, Y. Fan, Z. Hu, *ACS Catal.* **2014**, *4*, 613–621.
[5] X. Zhou, J. Ji, D. Wang, X. Duan, G. Qian, D. Chen, X. Zhou, *Chem. Commun.* **2015**, *51*, 8853–8856.
[6] a) U. Olsbye, S. Svelle, M. Bjørgen, P. Beato, T. V. M. Janssens, F. Joensen, S. Bordiga, K. P. Lillerud, *Angew. Chem. Int. Ed.* **2012**, *51*, 5810–5831; *Angew. Chem.* **2012**, *124*, 5910–5933; b) P. Tian, Y. Wei, M. Ye, Z. Liu, *ACS Catal.* **2015**, *5*, 1922–1938.
[7] a) J. Bao, J. He, Y. Zhang, Y. Yoneyama, N. Tsubaki, *Angew. Chem. Int. Ed.* **2008**, *47*, 353–356; *Angew. Chem.* **2008**, *120*, 359–362; b) J. Kang, K. Cheng, L. Zhang, Q. Zhang, J. S. Ding, W. Hua, Y. Lou, Q. Zhai, Y. Wang, *Angew. Chem. Int. Ed.* **2011**, *50*, 5200–5203; *Angew. Chem.* **2011**, *123*, 5306–5309; c) S. Sartipi, K. M. Makkee, F. Kapteijn, J. Gascon, *Catal. Sci. Technol.* **2014**, *4*, 893–907; d) X. Peng, K. Cheng, J. Kang, B. Gu, X. Yu, Q. Zhang, Y. Wang, *Angew. Chem. Int. Ed.* **2015**, *54*, 4553–4556; *Angew. Chem.* **2015**, *127*, 4636–4639.
[8] a) K. Fujimoto, H. Saima, H. Tominaga, *J. Catal.* **1985**, *94*, 16–23; b) Q. Zhang, X. Li, K. Asami, S. Asaoka, K. Fujimoto, *Fuel Process. Technol.* **2004**, *85*, 1139–1150; c) X. Ma, Q. Ge, J. Ma, H. Xu, *Fuel Process. Technol.* **2013**, *109*, 1–6.
[9] a) M. He, J. G. Ekeret, *J. Catal.* **1984**, *87*, 381–388; b) K. D. Jung, A. T. Bell, *J. Catal.* **2000**, *193*, 207–223.
[10] R. J. Kokes, A. L. Dent, C. C. Chang, L. T. Dixon, *J. Am. Chem. Soc.* **1972**, *94*, 4429–4436.
[11] S. Senger, L. Radom, *J. Am. Chem. Soc.* **2000**, *122*, 2613–2620.
[12] J. Zečević, G. Vanbutsele, K. P. de Jong, J. A. Martens, *Nature* **2015**, *528*, 245–248.

Received: February 2, 2016